Gravitational-wave cutoff frequencies of tidally disruptive neutron star-black hole binary mergers

Francesco Pannarale,[1,*] Emanuele Berti,[2,3] Koutarou Kyutoku,[4] Benjamin D. Lackey,[5,6] and Masaru Shibata[7]

[1]*School of Physics and Astronomy, Cardiff University, The Parade, Cardiff CF24 3AA, United Kingdom*
[2]*Department of Physics and Astronomy, The University of Mississippi, University, Mississippi 38677, USA*
[3]*CENTRA, Departamento de Física, Instituto Superior Técnico, Universidade de Lisboa,*
Avenida Rovisco Pais 1, 1049 Lisboa, Portugal
[4]*Interdisciplinary Theoretical Science (iTHES) Research Group, RIKEN, Wako, Saitama 351-0198, Japan*
[5]*Department of Physics, Princeton University, Princeton, New Jersey 08544, USA*
[6]*Department of Physics, Syracuse University, Syracuse, New York 13244, USA*
[7]*Yukawa Institute for Theoretical Physics, Kyoto University, Kyoto 606-8502, Japan*

Tidal disruption has a dramatic impact on the outcome of neutron star–black hole mergers. The phenomenology of these systems can be divided in three classes: nondisruptive, mildly disruptive, and disruptive. The cutoff frequency of the gravitational radiation produced during the merger (which is potentially measurable by interferometric detectors) is very different in each regime, and when the merger is disruptive it carries information on the neutron star equation of state. Here we use semianalytical tools to derive a formula for the critical binary mass ratio $Q = M_{BH}/M_{NS}$ below which mergers are disruptive as a function of the stellar compactness $\mathcal{C} = M_{NS}/R_{NS}$ and the dimensionless black hole spin χ. We then employ a new gravitational waveform amplitude model, calibrated to 134 general relativistic numerical simulations of binaries with black hole spin (anti-)aligned with the orbital angular momentum, to obtain a fit to the gravitational-wave cutoff frequency in the disruptive regime as a function of $\mathcal{C}$, Q, and χ. Our findings are important to build gravitational-wave template banks, to determine whether neutron star–black hole mergers can emit electromagnetic radiation (thus helping multimessenger searches), and to improve event rate calculations for these systems.

I. INTRODUCTION

The merger of black holes (BHs) and neutron stars (NSs) is one of the most violent events in the Universe. Coalescing NS-BH systems are among the leading candidate sources for upcoming interferometric gravitational-wave (GW) detectors such as the Advanced Laser Interferometer Gravitational-Wave Observatory (LIGO) [1,2], Virgo [3], the Kamioka Gravitational wave detector (KAGRA) [4,5], and LIGO-India [6]. GW observations of NS-BH mergers may provide information on the NS equation of state (EOS) [7,8] and on the underlying theory of gravity [9]. NS-BH binaries are also short-hard gamma-ray burst (SGRB) progenitor candidates [10]. If the NS is tidally disrupted during the merger, a hot disk with mass $\gtrsim 0.01 M_\odot$ may form around the spinning remnant BH. A scenario where the BH-disk system launches a relativistic jet by releasing its gravitational energy via neutrino or electromagnetic (EM) radiation on a time scale $\lesssim 2$ s explains the duration, energetics, and estimated event rates of SGRBs [11,12]. During their merger, NS-BH binaries may also emit EM radiation isotropically—as opposed to beamed SGRB emission—when they eject unbound material. This material can be as massive as $\sim 0.1 M_\odot$

and have subrelativistic velocities of $\sim 0.2 - 0.3c$ [13], producing EM counterparts in the form of macronovæ/kilonovæ, powered by decay heat of unstable r-process elements and by nonthermal radiation from electrons accelerated at blast waves between the merger ejecta and the interstellar medium [14–20].

The features of GW emission from NS-BH binaries, as well as the plausibility of these systems being central SGRB engines and sites for EM radiation emission, in general, depend crucially on whether or not the NS is tidally disrupted. Only numerical simulations can assess this. Fortunately, with the enormous progress made over the last decade, numerical relativity has provided a clear picture of NS-BH GW emission and shed light on the processes leading to disk formation and mass ejection. Most of the GW emission occurs prior to the NS tidal disruption, if this happens at all, and before significant thermal effects take place. Further, magnetic fields appear to barely affect the GW signal. These circumstances imply that an ideal fluid-dynamics treatment with a cold EOS is appropriate to simulate the dynamical regime of interest for GW signals. A notable feature of these signals is that the cutoff frequency at which their amplitude damps due to the NS tidal disruption depends on the NS EOS. Hence, the cutoff frequency encodes information on the EOS itself, particularly when this is stiff [21–24].

*francesco.pannarale@ligo.org

Numerical simulations of compact binary mergers are still very resource intensive, which makes semianalytical models very valuable. Simulations and models are most advanced for BH-BH systems. Waveform models belong to two main classes: Fourier-domain phenomenological inspiral-merger-ringdown (IMR) models based on a post-Newtonian (PN) description of the early inspiral stage (PhenomA [25–27], PhenomB [28], PhenomC [29], and PhenomP [30]) and effective-one-body models tuned to BH-BH simulations [31–37]. NS-BH waveform models are far less developed [38–40], because long, accurate simulations are particularly hard to achieve and because the parameter space is larger. The outcome and aftermath of NS-NS and NS-BH binary simulations (as opposed to BH-BH ones) depend on several assumptions on currently underconstrained physics, such as the NS EOS, magnetic field configurations, and neutrino emission. The relatively high mass ratios in NS-BH systems cause both analytical

and numerical complications: the convergence of the PN approximation is slower than for NS-NS systems [41,42], initial data are hard to construct [43], and the simulations must track very different dynamical time scales. In fact, BH-BH GW templates are commonly used in NS-BH merger searches. Tidal disruption affects both the GW and EM emission of NS-BH binaries. For all these reasons, better models can directly improve GW template banks, determine whether NS-BH mergers can power SGRBs and emit EM radiation in general (thus helping multimessenger searches), and improve event rate calculations for these systems.

II. SIMULATIONS AND MODEL

At least two papers attempted a phenomenological description of the GWs emitted by NS-BH binaries. Lackey *et al.* [39] developed an analytic representation
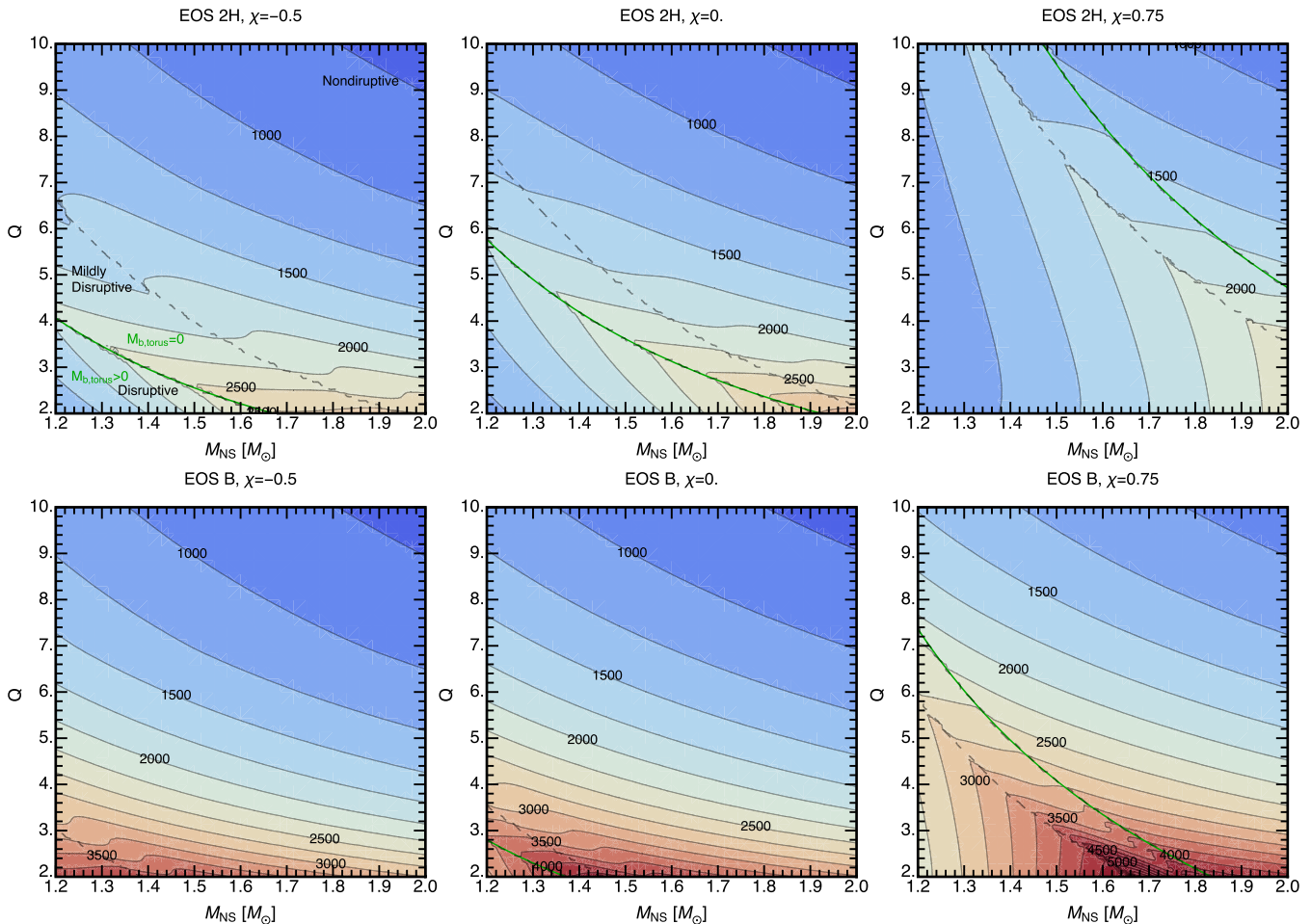

FIG. 1 (color online). The cutoff frequency $f_{\rm cut}$, as defined in Eq. (1), computed with our NS-BH GW amplitude model [38]. Each panel label specifies the NS EOS and the BH spin parameter χ used. The contour lines report $f_{\rm cut}$ in Hz and have a spacing of 250 Hz. The thick, green, continuous line is the location where the mass of the torus remnant $M_{\rm b,torus}$ vanishes. The two dashed lines in each panel divide the plane in three regions: a top-right region in which NS-BH coalescences are nondisruptive ($f_{\rm tide} \geq f_{\rm RD}$ and $M_{\rm b,torus} = 0$), a bottom-left one in which they are disruptive ($f_{\rm tide} < f_{\rm RD}$ and $M_{\rm b,torus} > 0$), and a middle region in which mildly disruptive coalescences occur ($f_{\rm tide} < f_{\rm RD}$ and $M_{\rm b,torus} = 0$, or $f_{\rm tide} \geq f_{\rm RD}$ and $M_{\rm b,torus} > 0$).

of the IMR waveform calibrated to 134 numerical wave-forms produced by the SACRA code [44] with the goal of assessing the measurability of the NS tidal deformability. The subset of simulations for nonspinning BHs was used by Pannarale *et al.* [40] to build a frequency domain phenomenological waveform *amplitude* model which was, at heart, a "distortion" of the PhenomC BH-BH model. This model relied on the fit of numerical-relativity results presented in [45] to compute the remnant torus mass $M_{\mathrm{b,torus}}$. It paid particular attention to the accuracy at high frequencies—where the EOS-related phenomenology takes place—and to the determination of the GW cutoff fre-quency. In units in which the total mass of the system is set to unity, let $h(f)$ be the Fourier transform of the GW signal, and f_{Max} the frequency at which $f^2 h(f)$ is maximum. We define f_{cut} ($> f_{\mathrm{Max}}$) as the frequency at which the dimen-sionless amplitude drops by one *e*-fold:

$$e f_{\mathrm{cut}} h(f_{\mathrm{cut}}) = f_{\mathrm{Max}} h(f_{\mathrm{Max}}). \qquad (1)$$

Figure 1 displays f_{cut} for a sample of BH spin parameters and for two piecewise polytropic EOS models (2H and B), chosen because they yield low- and high-compactness NSs, respectively (see [38]). This cutoff frequency is important to construct GW template banks for NS-BH searches: targeting NS-BH binaries with BH-BH templates termi-nated at a frequency $f_{\mathrm{term}} < f_{\mathrm{cut}}$ results in a signal-to-noise ratio loss; on the contrary, using $f_{\mathrm{term}} > f_{\mathrm{cut}}$ may penalize the template by degrading its chi-square test performance, as it lacks matter effects.

The companion paper [38] extends the work of [40] to NS-BH systems with a nonprecessing, spinning BH, using the full set of 134 hybrid waveforms constructed in [39]. These are based on simulations in which the NS matter at zero temperature is modeled via piecewise polytropic EOSs that mimic nuclear-theory-based EOSs with a small number of parameters [46]. The binary mass ratio takes the values $Q \in \{2, 3, 4, 5\}$ and the BH dimensionless spin parameter $\chi \in \{-0.5, 0, 0.25, 0.5, 0.75\}$. This parameter space cover-age allows our model to produce the most accurate prediction of cutoff frequencies for NS-BH GW signals, with relative errors below 10%, well below the errors one would obtain using either BH-BH models or the NS-BH model of [39]. The new NS-BH GW amplitude model used here, and detailed in Ref. [38], is adapted to the three possible fates of the binary (see also Fig. 1): (1) *non-disruptive*: the GW frequency at the onset of tidal dis-ruption $f_{\mathrm{tide}} \geq f_{\mathrm{RD}}$ (where f_{RD} is the BH remnant dominant ringdown frequency, calculated as in [47,48], and f_{tide} is the frequency at the onset of mass-shedding, determined as in [45]), and $M_{\mathrm{b,torus}}$, computed as in [45], vanishes, (2) *disruptive*: $f_{\mathrm{tide}} < f_{\mathrm{RD}}$ and $M_{\mathrm{b,torus}} > 0$, and (3) *mildly disruptive*: either $f_{\mathrm{tide}} < f_{\mathrm{RD}}$ and $M_{\mathrm{b,torus}} = 0$, or $f_{\mathrm{tide}} \geq f_{\mathrm{RD}}$ and $M_{\mathrm{b,torus}} > 0$. The BH ringdown does not contribute to the GW emission of disruptive mergers.

Ringdown radiation appears in mildly disruptive mergers, and looks similar to BH-BH mergers in nondisruptive cases. Disruptive mergers thus differ the most from BH-BH mergers, precisely because tidal effects are maximal. In these events, f_{cut} and the NS EOS have a strong link. To encompass all NS-BH binaries with a GW signal deviating from the BH-BH case, one must consider disruptive and mildly disruptive mergers; i.e., binaries above the top dashed curves in Fig. 1 must be discarded. The remaining set of binaries includes the $M_{\mathrm{b,torus}} = 0$ surface and, thus, all possible EM sources (within the approximations of the model).

III. PREDICTING THE FATE OF NS-BH MERGERS

The two dashed curves in the panels of Fig. 1 separate disruptive mergers (bottom-left region), nondisruptive mergers (top-right region), and mildly disruptive mergers (region in between the two lines). The green continuous line marks the locus of binaries for which $M_{\mathrm{b,torus}}$ goes to zero. Here we construct simple formulas to quickly determine the fate of a NS-BH coalescence. The contours in Fig. 1 that separate NS-BH binaries with a disruptive fate from those with a mildly disruptive or nondisruptive fate may be fitted in several ways as a function of the binary physical parameters. We find it best to fit the critical mass ratio Q_{D} *below* which mergers are classified as disruptive via a function of the form $Q_{\mathrm{D}} = Q_{\mathrm{D}}(\mathcal{C}, \chi)$. Fitting in terms of the NS compactness $\mathcal{C}$, rather than fixing an EOS and fitting in terms of the NS mass, allows us to use at the same time data produced with the two extreme EOSs B and 2H. This is evident in Fig. 2, where the boundaries between disruptive and mildly disruptive or nondisruptive binaries are shown in the $\mathcal{C}Q$ plane for initial BH spin parameter values $\chi \in \{-0.5, -0.25, 0., 0.25, 0.5, 0.75\}$: results for the 2H EOS (continuous) and the B EOS (dashed) overlay.
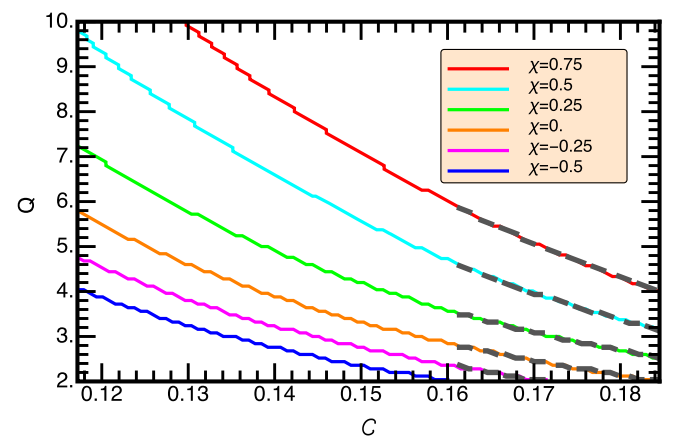

FIG. 2 (color online).   Boundaries separating disruptive mergers with $f_{\mathrm{tide}} < f_{\mathrm{RD}}$ and $M_{\mathrm{b,torus}} > 0$ (below each curve) from mildly disruptive and nondisruptive mergers (above each curve) for specific BH spin values indicated in the legend from top to bottom. Continuous (dashed gray) lines refer to EOS 2H (B).

TABLE I. Values of the coefficients of the fits in Eqs. (2)–(4). The number below each coefficient symbol must be multiplied by the corresponding power of 10 in square brackets. The f_{ijk}'s are expressed in units of $G = c =$ total mass $= 1$.

$a_{00}[10^1]$	$a_{10}[10^2]$	$a_{01}[10^1]$	$a_{20}[10^3]$	$a_{11}[10^2]$	$a_{02}[10^1]$	$a_{30}[10^3]$	$a_{21}[10^2]$	$a_{12}[10^1]$	$a_{03}[10^{-1}]$
4.59676	−6.68812	2.78668	3.56791	−2.79252	1.07053	−6.69647	7.55858	−5.51855	4.01679
	$a_0[10^1]$	$a_1[10^1]$	$a_2[10^1]$	$a_3[10^1]$	$b_0[10^1]$	$b_1[10^0]$	$b_2[10^1]$	$b_3[10^1]$	
	5.52167	4.05338	3.09804	−6.90163	−1.68616	−2.87849	−1.82097	1.36910	
$f_{000}[10^{-1}]$	$f_{100}[10^0]$	$f_{010}[10^{-2}]$	$f_{001}[10^{-2}]$	$f_{200}[10^1]$	$f_{020}[10^{-3}]$	$f_{002}[10^{-2}]$	$f_{110}[10^{-1}]$	$f_{101}[10^{-1}]$	$f_{011}[10^{-4}]$
1.38051	−2.36698	−3.07791	3.06474	1.19668	1.81262	4.31813	2.89424	−1.61434	9.30676
$f_{300}[10^1]$	$f_{030}[10^{-5}]$	$f_{003}[10^{-3}]$	$f_{210}[10^{-1}]$	$f_{120}[10^{-3}]$	$f_{201}[10^{-1}]$	$f_{102}[10^{-1}]$	$f_{021}[10^{-4}]$	$f_{012}[10^{-3}]$	$f_{111}[10^{-2}]$
−1.46271	−6.89872	−2.29830	2.73922	−4.69093	1.75728	−2.04964	5.52098	−5.79629	−9.09280

This is due to the fact that the criterion to determine whether a binary is disruptive or not depends on $M_{\text{b,torus}}$, and that the state-of-the-art model for $M_{\text{b,torus}}$ [45] depends only on $\mathcal{C}$ (i.e., it does not include higher-order, EOS-dependent effects). Quite independently of the EOS, the merger of an NS-BH binary will be disruptive whenever $Q < Q_{\text{D}}(\mathcal{C}, \chi)$, where the threshold is well fitted by

$$Q_{\text{D}} = \sum_{i,j=0}^{3} a_{ij}\mathcal{C}^i\chi^j, \qquad i+j \leq 3, \tag{2}$$

with coefficients reported in the first row of Table I. The relative errors between the data in Fig. 2 and our fit are below $\sim 4\%$ [38]. Similarly, the relation

$$Q_{\text{ND}} = \left(\sum_{i=0}^{3} a_i\chi^i\right) \exp\left[\left(\sum_{j=0}^{3} b_j\chi^j\right)\mathcal{C}\right], \tag{3}$$

with coefficient values listed in the second row of Table I, fits the boundary between nondisruptive and mildly disruptive mergers so that NS-BH systems with $Q < Q_{\text{ND}}(\mathcal{C}, \chi)$ are either disruptive or mildly disruptive. The maximum relative error between the data and the fit is $\sim 8\%$, and it is below 4.5% for 95% of the data points.

IV. CUTOFF FREQUENCY OF DISRUPTIVE MERGERS

Equation (2) allows us to determine when a binary is disruptive according to our classification; i.e., the mass-shedding happens early enough during the evolution for the merger to produce a remnant disk mass and the GW emission deviates significantly from the BH-BH case at high frequencies. We now wish to provide a simple formula to compute the cutoff frequency of the GW amplitude f_{cut} for disruptive mergers, as it carries information on the nuclear EOS and it may be valuable in building better GW template banks. To this end we consider EOS 2H, generate a set of 10^4 random disruptive mergers, compute f_{cut} for each NS-BH binary, and finally fit the resulting data. Disruptive mergers are selected as follows: we randomly sample parameters in the ranges $M_{\text{NS}}/M_\odot \in [1.2, 2.83]$, $Q \in [2, 10]$, $\chi \in [-0.5, 0.75]$; we verify whether the

sampled point corresponds to a disruptive binary, i.e. whether $f_{\text{tide}} < f_{\text{RD}}$ and $M_{\text{b,torus}} > 0$; we keep the point if it does; and we repeat the whole process until we have the desired 10^4 points. While the maximum NS mass for the 2H EOS is $\sim 2.83 M_\odot$, the maximum NS mass we obtain for the sample of disruptive NS-BH mergers is $\sim 2.28 M_\odot$. The resulting mass interval $M_{\text{NS}}/M_\odot \in [1.2, 2.28]$ corresponds to a compactness interval of $0.117 \leq \mathcal{C} \leq 0.221$. We then fit the data set with the function

$$f_{\text{cut}} = \sum_{i,j,k=0}^{3} f_{ijk}\mathcal{C}^i Q^j \chi^k, \qquad i+j+k \leq 3. \tag{4}$$

The resulting f_{ijk} values are reported in Table I. The relative errors between this fit and the data are typically below 1%: the relative error for 68%, 95%, and 99.7% of the points is 0.47%, 1.5%, and 4.9%, respectively.

As a consistency check, we draw a separate sample of 10^4 disruptive mergers, and, for each binary, compute f_{cut} and the relative error yielded by Eq. (4). This time we use EOS B, which has a maximum NS mass of $\sim 2M_\odot$. The compactness now ranges from 0.161 to 0.225. Quite remarkably, the maximum relative error is 2.2%; the relative error of 97.6% of the points is below the percent level. This check implies that Eq. (4) is to a good approximation EOS-independent, at least within the parameter space where our model was calibrated and applied.

V. SUMMARY AND DISCUSSION

In this paper we used a recently developed semianalytical GW amplitude model for NS-BH mergers [38] to construct simple fits for (i) the critical binary mass ratio Q_{D} below which the merger is disruptive [Eq. (2)] and its GW emission deviates significantly from a BH-BH–like behavior, (ii) the critical binary mass ratio Q_{ND} below which the merger is either disruptive or mildly disruptive [Eq. (3)] (which can be viewed as a necessary but not sufficient condition to generate an EM counterpart and may, thus, be used to determine which binaries are plausible targets for multimessenger searches targeting GWs and EM/neutrino emission), and (iii) the cutoff frequency f_{cut} for disruptive mergers as a function of the initial binary parameters $\mathcal{C}$, Q,

and χ [Eq. (4)]. This can be used to maximize the recovered signal-to-noise ratio and chi-square test performance of BH-BH templates in NS-BH searches. The cutoff frequency can also be used to constrain the NS EOS [21–24,49–51]. Our fit suggests that measurements of $\mathcal{C}$, Q, or χ from the inspiral radiation (see e.g. [52,53]) could improve the resulting constraints on the EOS.

The non-negligible eccentricity of the initial data used for the NS-BH simulations underlying our model, the limited duration and finite numerical resolution of the simulations, and the fitting errors all limit the accuracy of f_{cut} to a few percent and, therefore, introduce systematic errors. These errors are expected to increase as $Q \to Q_{\mathrm{D}}$ and when our fits are extrapolated beyond the region where the model and fits were tuned. More importantly, it is necessary to extend our model to precessing binaries [54]. We plan to address these issues in future work.

[1] J. Aasi *et al.* (LIGO Scientific), Classical Quantum Gravity **32**, 074001 (2015).
[2] and the LIGO Scientific Collaboration, Classical Quantum Gravity **27**, 084006 (2010).
[3] F. Acernese *et al.* (VIRGO Collaboration), Classical Quantum Gravity **32**, 024001 (2015).
[4] K. Somiya (KAGRA Collaboration), Classical Quantum Gravity **29**, 124007 (2012).
[5] Y. Aso, Y. Michimura, K. Somiya, M. Ando, O. Miyakawa, T. Sekiguchi, D. Tatsumi, and H. Yamamoto, Phys. Rev. D **88**, 043007 (2013).
[6] IndIGO, website: http://www.gw-indigo.org/ (2012).
[7] F. Pannarale, L. Rezzolla, F. Ohme, and J. S. Read, Phys. Rev. D **84**, 104017 (2011).
[8] J. S. Read, C. Markakis, M. Shibata, K. Uryu, J. D. Creighton, and J. Friedman, Phys. Rev. D **79**, 124033 (2009).
[9] E. Berti *et al.*, arXiv:1501.07274.
[10] B. Paczynski, Acta Astronomica **41**, 257 (1991).
[11] E. Nakar, Phys. Rep. **442**, 166 (2007).
[12] E. Berger, Annu. Rev. Astron. Astrophys. **52**, 43 (2014).
[13] K. Kyutoku, K. Ioka, H. Okawa, M. Shibata, and K. Taniguchi, Phys. Rev. D **92**, 044028 (2015).
[14] L.-X. Li and B. Paczyński, Astrophys. J. **507**, L59 (1998).
[15] S. R. Kulkarni, arXiv:astro-ph/0510256.
[16] B. D. Metzger, G. Martínez-Pinedo, S. Darbha, E. Quataert, A. Arcones, D. Kasen, R. Thomas, P. Nugent, I. V. Panov, and N. T. Zinner, Mon. Not. R. Astron. Soc. **406**, 2650 (2010).
[17] E. Nakar and T. Piran, Nature (London) **478**, 82 (2011).
[18] H. Takami, K. Kyutoku, and K. Ioka, Phys. Rev. D **89**, 063006 (2014).
[19] S. Kisaka, K. Ioka, and H. Takami, Astrophys. J. **802**, 119 (2015).

[20] B. Yang, Z.-P. Jin, X. Li, S. Covino, X.-Z. Zheng, K. Hotokezaka, Y.-Z. Fan, T. Piran, and D.-M. Wei, Nat. Commun. **6**, 7323 (2015).
[21] M. Shibata, K. Kyutoku, T. Yamamoto, and K. Taniguchi, Phys. Rev. D **79**, 044030 (2009).
[22] V. Ferrari, L. Gualtieri, and F. Pannarale, Phys. Rev. D **81**, 064026 (2010).
[23] K. Kyutoku, M. Shibata, and K. Taniguchi, Phys. Rev. D **82**, 044049 (2010).
[24] K. Kyutoku, H. Okawa, M. Shibata, and K. Taniguchi, Phys. Rev. D **84**, 064018 (2011).
[25] P. Ajith, S. Babak, Y. Chen, M. Hewitson, B. Krishnan *et al.*, Classical Quantum Gravity **24**, S689 (2007).
[26] P. Ajith, S. Babak, Y. Chen, M. Hewitson, B. Krishnan *et al.*, Phys. Rev. D **77**, 104017 (2008).
[27] P. Ajith, Classical Quantum Gravity **25**, 114033 (2008).
[28] P. Ajith, M. Hannam, S. Husa, Y. Chen, B. Bruegmann *et al.*, Phys. Rev. Lett. **106**, 241101 (2011).
[29] L. Santamaría, F. Ohme, P. Ajith, B. Bruegmann, N. Dorband *et al.*, Phys. Rev. D **82**, 064016 (2010).
[30] M. Hannam, P. Schmidt, A. Bohé, L. Haegel, S. Husa, F. Ohme, G. Pratten, and M. Pürrer, Phys. Rev. Lett. **113**, 151101 (2014).
[31] A. Taracchini, Y. Pan, A. Buonanno, E. Barausse, M. Boyle, T. Chu, G. Lovelace, H. P. Pfeiffer, and M. A. Scheel, Phys. Rev. D **86**, 024011 (2012).
[32] T. Damour, A. Nagar, and S. Bernuzzi, Phys. Rev. D **87**, 084035 (2013).
[33] T. Damour, A. Nagar, and M. Trias, Phys. Rev. D **83**, 024006 (2011).
[34] F. Ohme, M. Hannam, and S. Husa, Phys. Rev. D **84**, 064029 (2011).
[35] Y. Pan, A. Buonanno, A. Taracchini, L. E. Kidder, A. H. Mroué, H. P. Pfeiffer, M. A. Scheel, and B. Szilágyi, Phys. Rev. D **89**, 084006 (2014).

[36] A. Taracchini *et al.*, Phys. Rev. D **89**, 061502 (2014).

[37] B. Szilágyi, J. Blackman, A. Buonanno, A. Taracchini, H. P. Pfeiffer, M. A. Scheel, T. Chu, L. E. Kidder, and Y. Pan, Phys. Rev. Lett. **115**, 031102 (2015).

[38] F. Pannarale, E. Berti, K. Kyutoku, B. D. Lackey, and M. Shibata, Phys. Rev. D **92**, 084050 (2015).

[39] B. D. Lackey, K. Kyutoku, M. Shibata, P. R. Brady, and J. L. Friedman, Phys. Rev. D **89**, 043009 (2014).

[40] F. Pannarale, E. Berti, K. Kyutoku, and M. Shibata, Phys. Rev. D **88**, 084011 (2013).

[41] E. Berti, S. Iyer, and C. M. Will, Phys. Rev. D **77**, 024019 (2008).

[42] A. Buonanno, B. Iyer, E. Ochsner, Y. Pan, and B. Sathyaprakash, Phys. Rev. D **80**, 084043 (2009).

[43] K. Kyutoku, M. Shibata, and K. Taniguchi, Phys. Rev. D **90**, 064006 (2014).

[44] T. Yamamoto, M. Shibata, and K. Taniguchi, Phys. Rev. D **78**, 064054 (2008).

[45] F. Foucart, Phys. Rev. D **86**, 124007 (2012).

[46] J. S. Read, B. D. Lackey, B. J. Owen, and J. L. Friedman, Phys. Rev. D **79**, 124032 (2009).

[47] F. Pannarale, Phys. Rev. D **88**, 104025 (2013).

[48] F. Pannarale, Phys. Rev. D **89**, 044045 (2014).

[49] M. Vallisneri, Phys. Rev. Lett. **84**, 3519 (2000).

[50] V. Ferrari, L. Gualtieri, and F. Pannarale, Classical Quantum Gravity **26**, 125004 (2009).

[51] K. Taniguchi, T. W. Baumgarte, J. A. Faber, and S. L. Shapiro, Phys. Rev. D **77**, 044003 (2008).

[52] R. O'Shaughnessy, B. Farr, E. Ochsner, H.-S. Cho, V. Raymond, C. Kim, and C.-H. Lee, Phys. Rev. D **89**, 102005 (2014).

[53] M. Hannam, D. A. Brown, S. Fairhurst, C. L. Fryer, and I. W. Harry, Astrophys. J. **766**, L14 (2013).

[54] K. Kawaguchi, K. Kyutoku, H. Nakano, H. Okawa, M. Shibata, and K. Taniguchi, Phys. Rev. D **92**, 024014 (2015).